Supporting Information

Luminescent Cyclic Trinuclear Coinage Metal Complexes with Aggregation-Induced Emission (AIE) Performance

Yuan Tian[a], Zhao-Yang Wang*[a], Shuang-Quan Zang*[a], Dan Li*[b] and Thomas C. W. Mak[a,c]

[a]College of Chemistry and Molecular Engineering, Zhengzhou University, Zhengzhou 450001, China

[b]College of Chemistry and Materials Science, Jinan University, Guangzhou 510632, China

[c]Department of Chemistry and Center of Novel Functional Molecules, The Chinese University of Hong Kong, Shatin, New Territories, Hong Kong

E-mail: zangsqzg@zzu.edu.cn, wangzy@zzu.edu.cn, danli@jnu.edu.cn

Table of Contents

Experimental section

Materials: All reagents and solvents were commercially available reagent grade and were used without any additional purification.

Characterization: UV-vis absorption spectra were recorded with a U-2000 spectrophotometer. ^{13}C NMR and ^{1}H NMR were carried out on a Bruker 400 spectrometer. Thermogravimetric analysis (TGA) of the compounds were performed on a SDT 2960 thermal analyzer from room temperature to 400 ^{o}C at a heating rate of 10 $^{o}C \cdot min^{-1}$ under N_2 atmosphere.

General procedures:

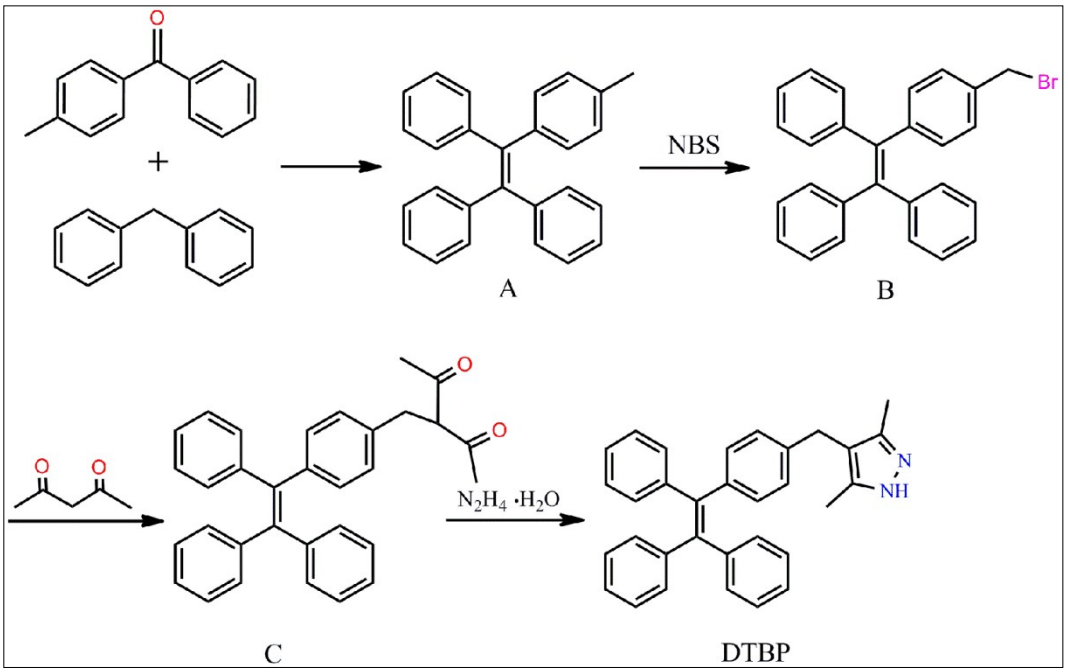

Figure S1. Schematic represented the preparation route of *3,5-dimethyl-4-(4-(1,2,2-triphenylvinyl)benzyl)-1H-pyrazole* (DTBP).

Synthesis of *1-(4-Methylphenyl)-l,2,2-triphenylethylene* (A): The synthesis of **A** was prepared as described in literature.[1-4] To a solution of diphenylmethane (2.02 g, 12 mmol) in dry THF (20 mL) was added 4 mL of a 2.5 M solution of *n*-butyllithium (10 mmol) in hexane at 0 °C under nitrogen. The resulting orange-red solution was stirred for 1 h at this temperature. 4-Methylbenzophenone (1.77 g, 9 mmol) was then added and the reaction mixture was warmed to room temperature and stirred for another 6 h. The reaction was quenched by addition of 10% aqueous ammonium chloride solution. The solution was extracted with dichloromethane (3×50 mL), and the combined organic layers were washed with a saturated brine solution and dried over anhydrous $MgSO_4$. The solvent was evaporated, and the resulting crude alcohol was dissolved in 80 mL of toluene in a 150 mL round-bottom flask fitted with a Dean-Stark trap. A catalytic amount of ptoluenesulphonic acid (342 mg, 1.8 mmol) was added, and the mixture was refluxed for 4 h and cooled to room temperature. The toluene layer was washed with 10% $NaHCO_3$ aqueous solution and dried over anhydrous $MgSO_4$. After evaporating the solvent and recrystallization from dichloromethane and methanol, white powder was obtained (2.77 g, 89%).

Synthesis of *1-[4-(Bromomethyl)phenyl]-1,2,2-diphenylethene* (B): The synthesis of **B** was prepared also as described in literature.[1-4] 1-(4-Methylphenyl)-l,2,2-triphenylethylene (1.73 g, 5.0 mmol), NBS (0.98 g, 5.5 mmol), and BPO (20 mg, 0.1 mmol) in CCl_4 (70 mL) was heated at 80 °C for 24 h. Then the reaction mixture was cooled to room temperature and filtered. After the solvent was evaporated, the crude product was purified by silica gel column chromatography using petroleum ether as eluent to give white solid in 56% yield (1.19 g). ^{1}H NMR ($CDCl_3$, 400 MHz): δ = 4.43 (s, 2H), 7.01-7.16 (m, 19H).

Synthesis of *3-(4-(1,2,2-triphenylvinyl)benzyl)pentane-2,4-dione* (C): Sodium (0.056 g, 2.45 mmol) was dissolved in *tert*-butyl alcohol (50 mL). To this solution, 2,4-pentanedione (0.265 g, 2.65 mmol), 1-(bromomethyl)-4-(1,2,2-triphenylethenyl)benzene (1.04 g, 2.45 mmol) and KI (0.25 g) were added successively. The mixture was refluxed for 36 h under nitrogen. White precipitate was obtained after *tert*-butyl alcohol was removed with rotary evaporation, which was then dissolved in $CHCl_3$, and washed with water for several times to remove inorganic salts. The resulted $CHCl_3$ solution was dried by anhydrous magnesium sulfate. After filtered, the solution was rotary evaporated to give a yellow oily product.

Synthesis of *3,5-dimethyl-4-(4-(1,2,2-triphenylvinyl)benzyl)-1H-pyrazole* (DTBP): To the above-obtained $CHCl_3$ solution (50 mL) of diketone was added slowly a methanol solution (8 mL) of hydrazine (80% $N_2H_4 \cdot H_2O$, 141.9 μL, 2.92 mmol). The mixture was refluxed for 12 h and then the solvent was evaporated under reduced pressure. The residue dissolved in ether and washed with water for several times, and dried over anhydrous magnesium sulfate and evaporated to afford the yellow product. Yield: 83%. ^{1}H NMR ($CDCl_3$, 400 MHz): δ = 2.03 (s, 6H), 3.68 (s, 2H), 6.86-7.11 (m, 19H); ^{13}C NMR ($CDCl_3$, 400 MHz): δ = 143.89, 143.79, 143.75, 141.35, 140.84, 140.70, 138.92, 131.36, 127.65, 126.40, 126.38, 126.35, 114.25, 28.88, 11.06.

Synthesis of Au_3: A CH_2Cl_2 solution (4 mL) of Chloro(tetrahydrothiophene)gold (I) (49 mg, 0.15 mmol) was mixed with a CH_2Cl_2 solution (3 mL) of DTBP (66 mg, 0.15 mmol), then Et_3N (0.2 mmol) and CH_3CN (3 mL) was added. Stirred for 1 min, the solution became cloudy. After filtrate, the residue was washed with MeOH. Later, the precipitate was dissolved in $CHCl_3$ solution. Colorless crystals were obtained by slow diffusion of *n*-hexane into a $CHCl_3$ solution within two days. ^{1}H NMR ($CDCl_3$, 400 MHz): δ = 2.11 (s, 18H), 3.66 (s, 6H), 6.85-7.10 (m, 57H) Elemental analysis calcd. (%) for $C_{96}H_{81}N_6Au_3$ (1909.56): C 60.38; H 4.27; N 4.40; found: C 60.44; H 4.11; N 4.38.

Synthesis of Ag_3: It was prepared in the similar fashion to **Au_3**. The stoichiometry of the reagents are $AgNO_3$ (25 mg, 0.15 mmol), DTBP (66.0 mg, 0.15 mmol), Et_3N (0.2 mmol). ^{1}H NMR ($CDCl_3$, 400 MHz): δ = 2.03 (s, 18H), 3.68 (s, 6H), 6.86-7.11 (m, 57H) Elemental analysis calcd. (%) for $C_{96}H_{81}N_6Ag_3$ (1642.27): C 70.21; H 4.97; N 5.11; found: C 70.16; H 4.71; N 5.01.

Synthesis of Cu_3: Cu_3 was prepared in the similar fashion to **Ag_3** by replacing $AgNO_3$ with CuI (28 mg, 0.15 mmol). ^{1}H NMR ($CDCl_3$, 400 MHz): δ = 2.19 (s, 18H), 3.69 (s, 6H), 6.87-7.14 (m, 57H) Elemental analysis calcd. (%) for $C_{96}H_{81}N_6Cu_3$ (1509.28): C 76.39; H 5.41; N 5.56; found: C 76.49; H 5.38; N 5.74.

X-ray Crystallography

Single-crystal X-ray diffraction measurements of **Au_3** and **Cu_3** were performed on a Rigaku XtaLAB Pro diffractometer with Cu–Kα radiation (λ = 1.54178 Å) at 293 K and 150 K, respectively. **Ag_3** was measured with Mo–Kα radiation (λ = 0.71073 Å) at 200 K. Data collection and reduction were performed using the program CrysAlisPro.[5] All the structures were solved with direct methods (*SHELXS*)[6] and refined by full-matrix least squares on F^2 using *OLEX2*,[7] which utilizes the *SHELXL*-2015 module.[8] All the atoms were refined anisotropically, hydrogen atoms were placed in calculated positions refined using idealized geometries and assigned fixed isotropic displacement parameters. A satisfactory disorder model for the solvent molecules was not found in **Au_3** and **Ag_3**, therefore the *OLEX2* Solvent Mask routine (*PLATON/SQUEEZE*)[9] was used to mask out the disordered density.

The detailed information of the crystal data, data collection and refinement results for all compounds are summarized in Table 1.

Luminescence measurements

Luminescence measurements were carried out using a HORIBA FluoroLog-3 fluorescence spectrometer. Luminescence decays were measured on HORIBA Scientific Fluorolog-3 spectrofluorometer equipped with a 370 nm-laser, operating in time-correlated single photon counting mode (TCSPC) with a resolution time of 200 ps. The photoluminescent quantum efficiency in powder form was measured using an integrating sphere on a HORIBA Scientific Fluorolog-3 spectrofluorometer.

Powder X-ray diffraction (PXRD)

PXRD patterns of the compounds were collected at room temperature in air on a X'Pert PRO diffractometer (Cu-Kα). PXRD data for those with mother liquid were collected using Bruker D8 Advance diffractometer (Cu-Kα), during which the samples were packed with a small quantity of mother liquid.

Supplementary Figures

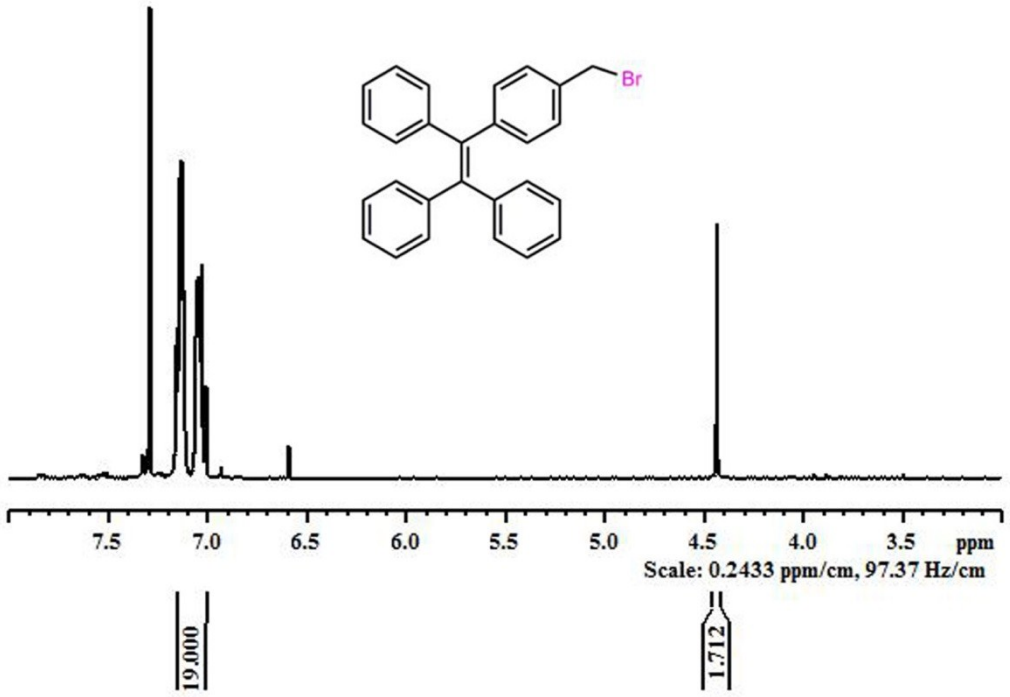

Figure S2.[1]H NMR spectrum of *1-[4-(Bromomethyl)phenyl]-1,2,2-diphenylethene* (B).

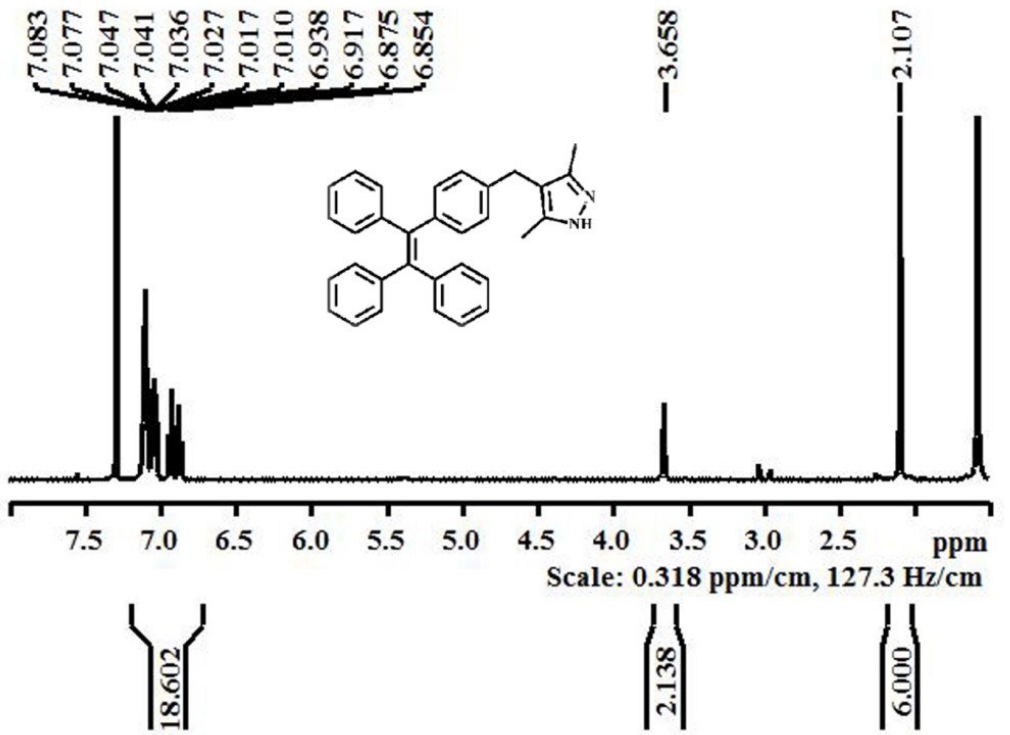

Figure S3.[1]H NMR spectrum of DTBP ligand.

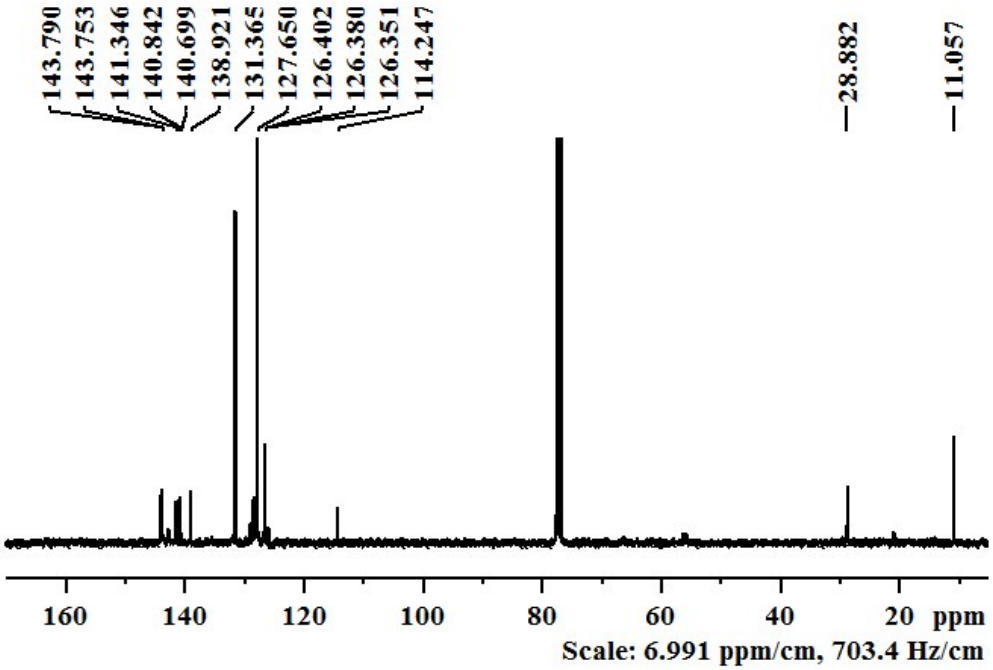

Figure S4.[13]C NMR spectrum of DTBP ligand.

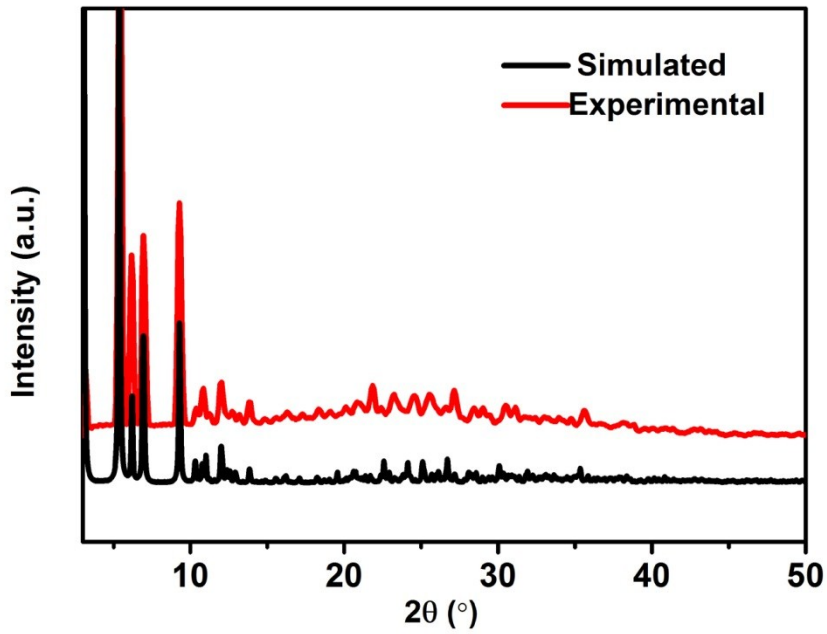

Figure S5. Experimental PXRD pattern of $\mathbf{Au_3}$ at room temperature compared to the simulated phase.

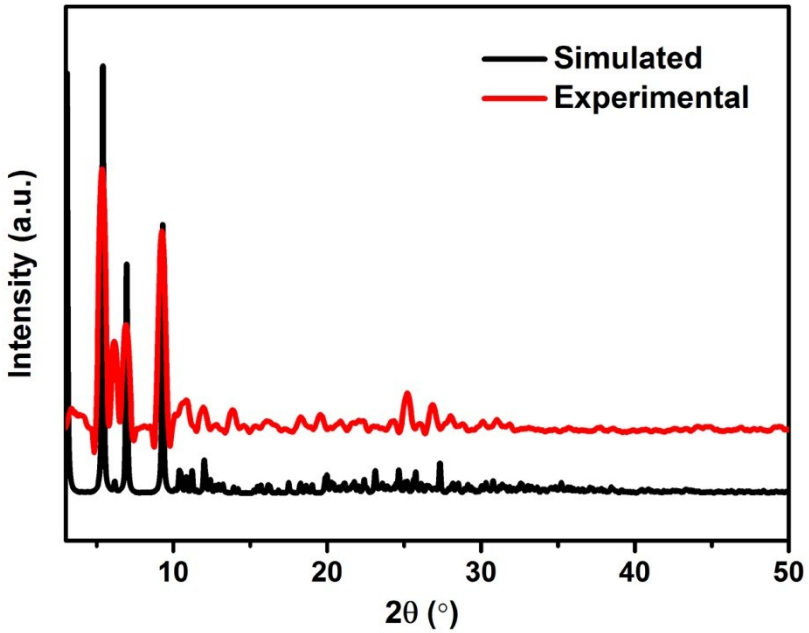

Figure S6. Experimental PXRD pattern of Ag_3 at room temperature compared to the simulated phase.

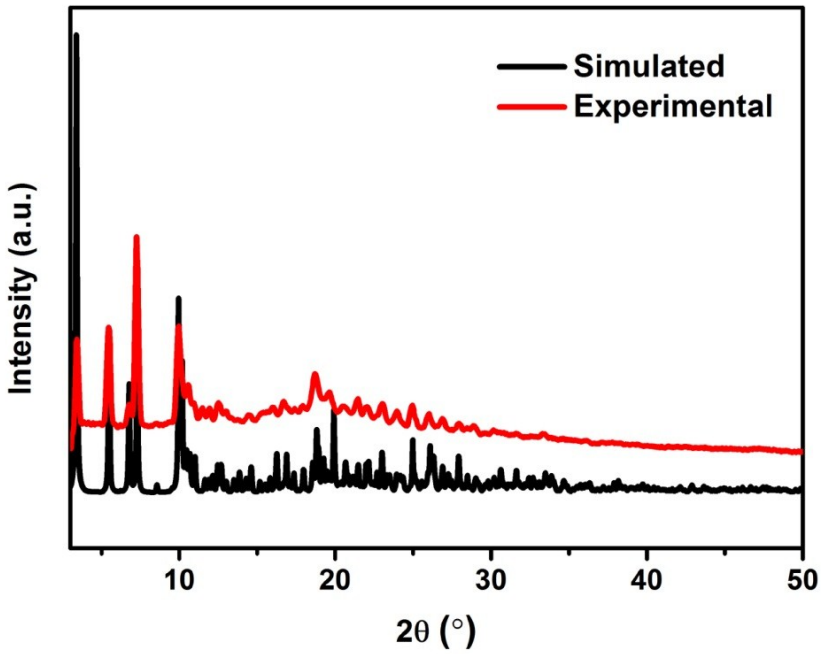

Figure S7. Experimental PXRD pattern of Cu_3 at room temperature compared to the simulated phase.

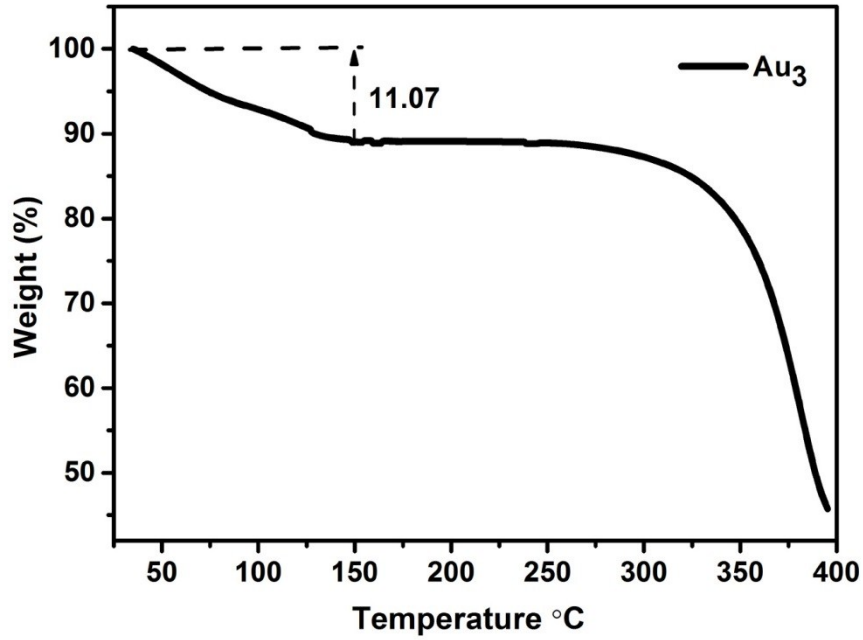

Figure S8. The TGA curve for **Au_3** showed 11.07% weight loss which corresponding to about 1 $CHCl_3$ and 1 CH_2Cl_2 molecules.

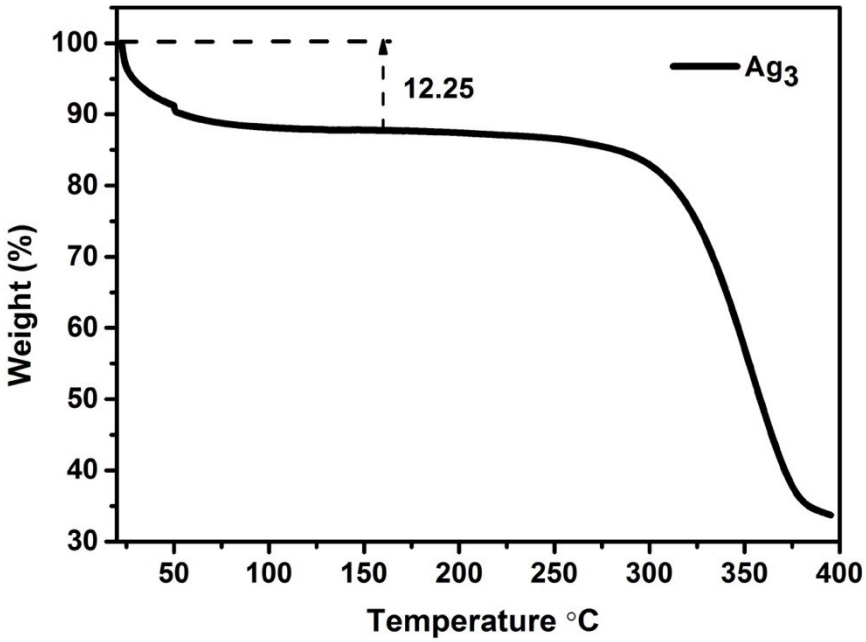

Figure S9. The TGA curve for **Ag_3** showed 12.25% weight loss which corresponding to about 2 $CHCl_3$ molecules.

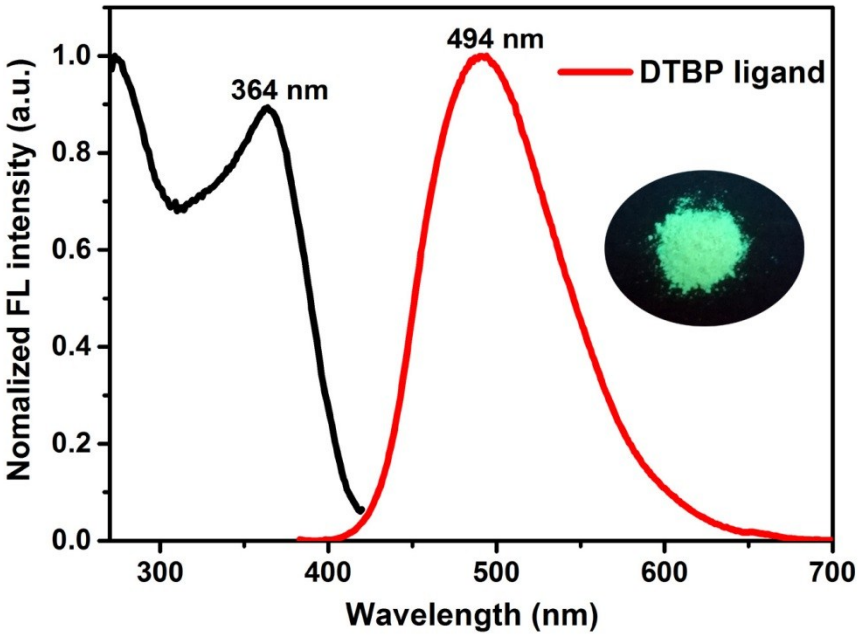

Figure S10. The fluorescence spectrum of DTBP. Inset: photograph of DTBP under 365 nm irradiation.

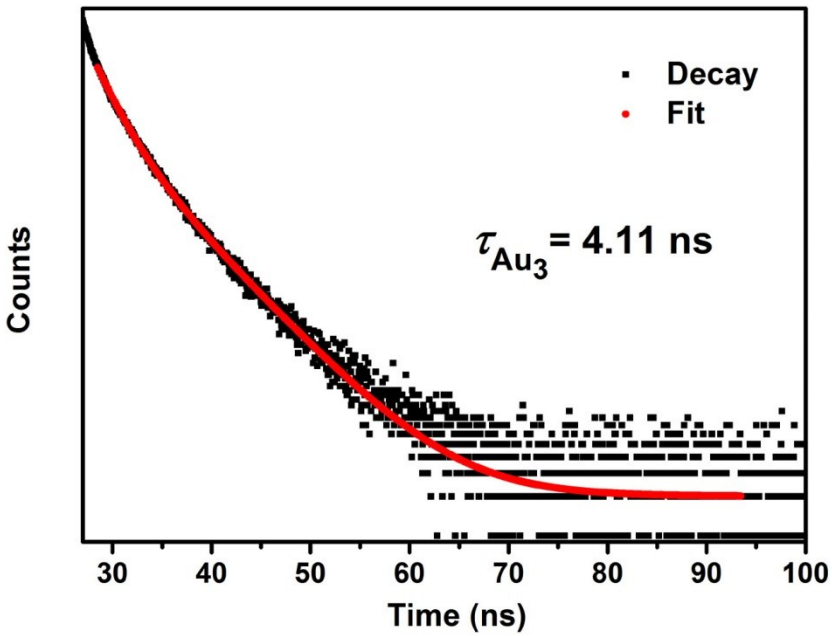

Figure S11. Photoluminescence decay profile of $\mathbf{Au_3}$ using 370 NanoLed under ambient conditions.

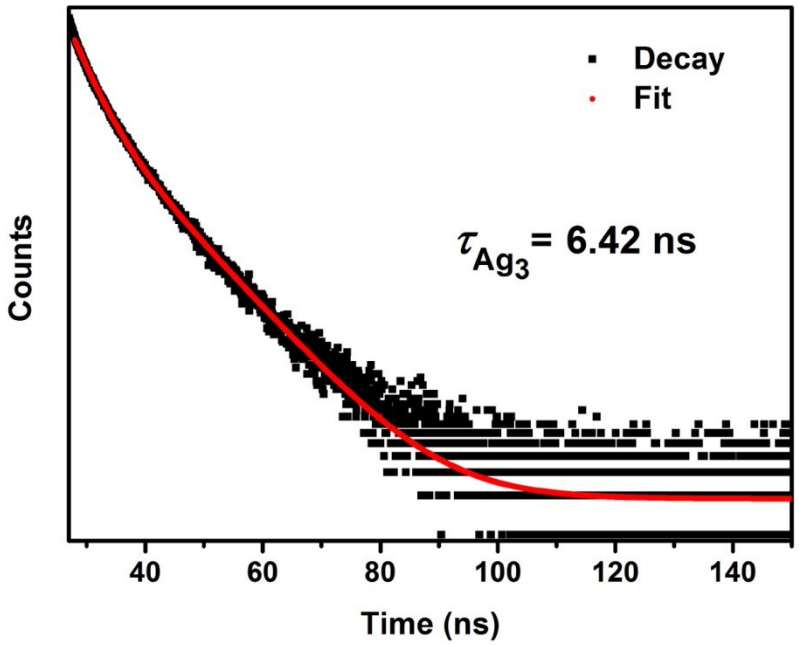

Figure S12. Photoluminescence decay profile of $\mathbf{Ag_3}$ using 370 NanoLed under ambient conditions.

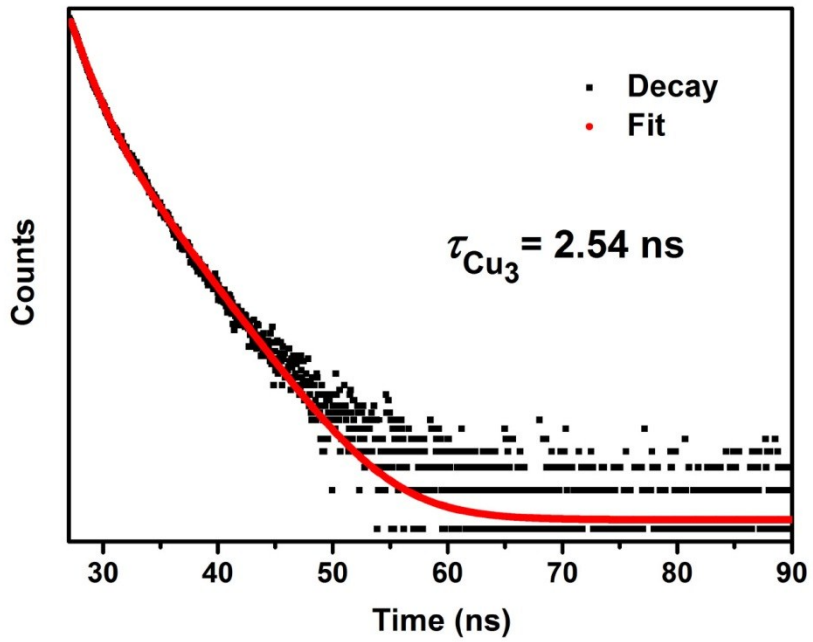

Figure S13. Photoluminescence decay profile of $\mathbf{Cu_3}$ using 370 NanoLed under ambient conditions.

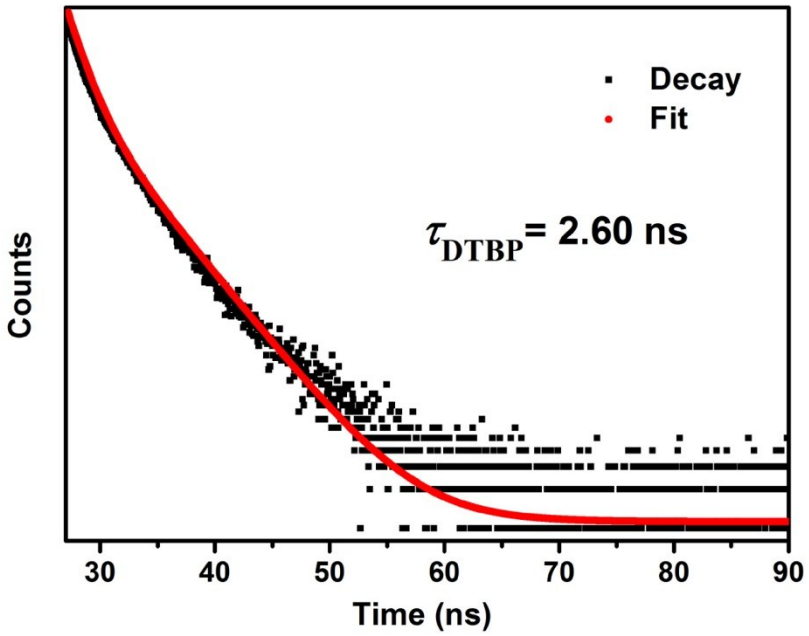

Figure S14. Photoluminescence decay profile of DTBP using 370 NanoLed under ambient conditions.

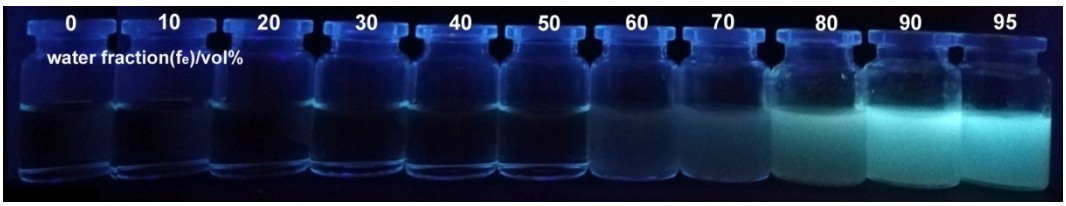

Figure S15. Photo images of DTBP ligand solutions in different water fraction, excited at 365 nm.

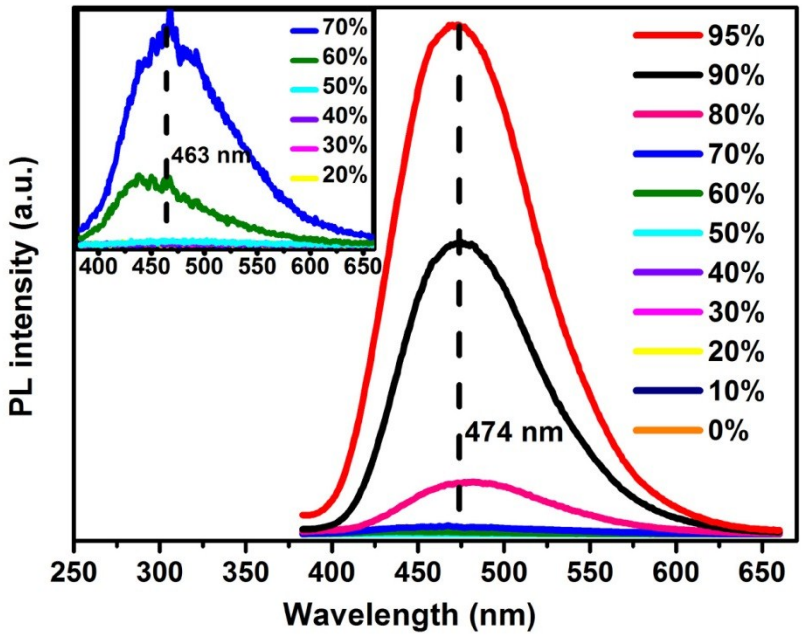

Figure S16. Photoemission spectra of DTBP in mixed solvents with different f_e (concentration: 1.36×10^{-3} M), excited at 363 nm.

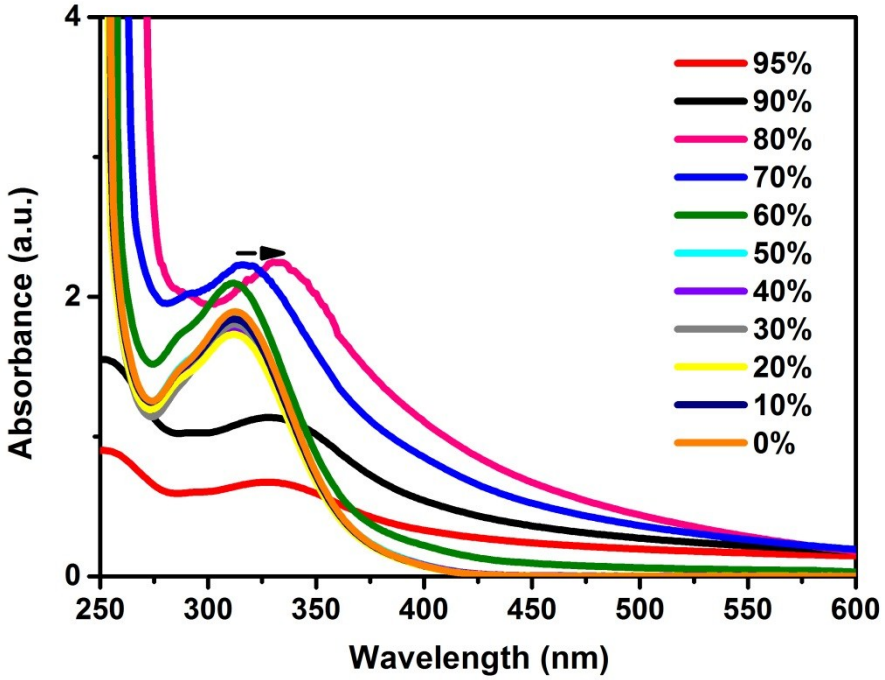

Figure S17. UV−vis absorption spectra of DTBP in mixed solvents with different f_e (concentration: 1.36×10^{-3} M), using a 1 mm thickness cuvette.

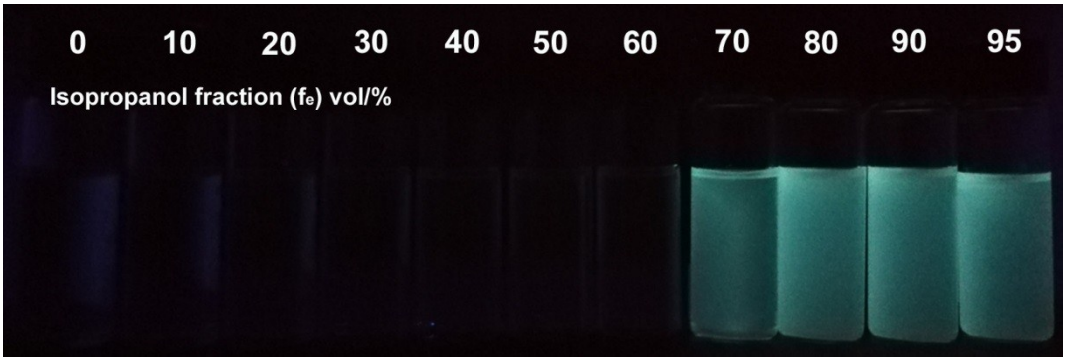

Figure S18. Digital photo of $\mathbf{Au_3}$ complexes (concentration: 2×10^{-4} M) in mixed solvents of tetrahydrofuran and ethanol with different f_e under UV light, excited at 365 nm.

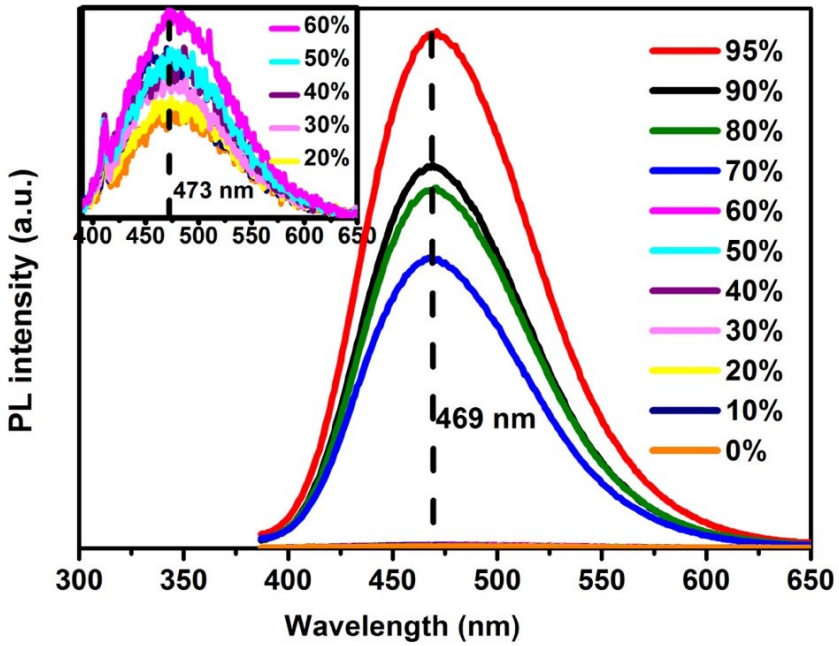

Figure S19. Photoemission spectra of $\mathbf{Au_3}$ in mixed solvents with different isopropanol fraction from 0% to 95% (concentration: 2×10^{-4} M), excited at 367 nm.

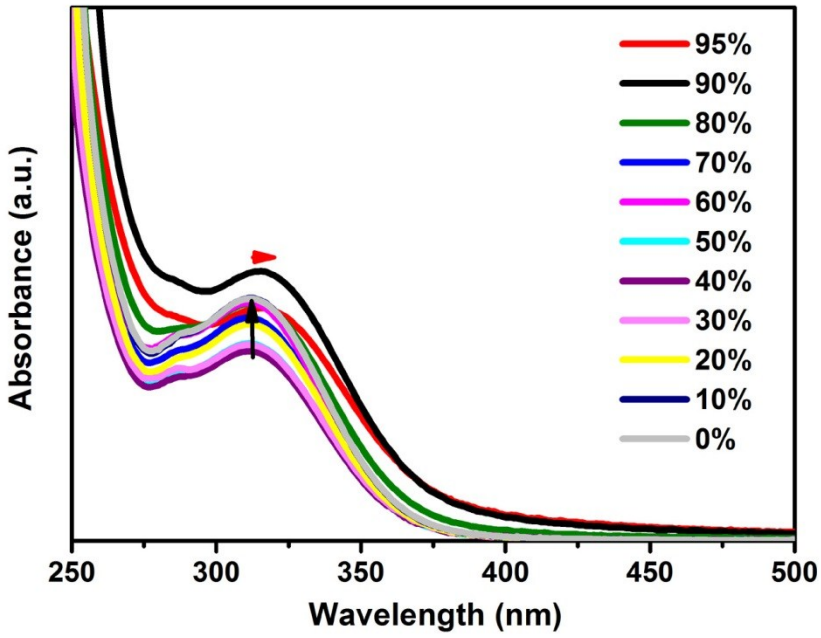

Figure S20. UV−vis absorption of **Au_3** in mixed solvents with different isopropanol fraction from 0% to 95% (concentration: 2×10^{-4} M), using a 1 mm thickness cuvette.

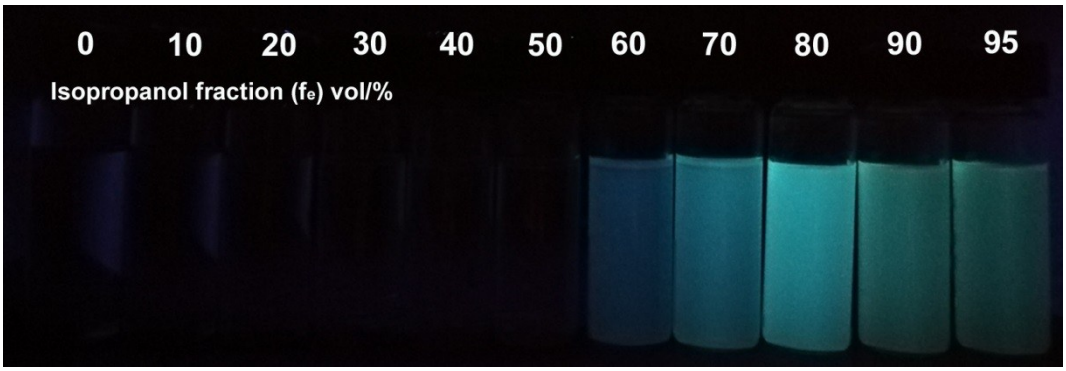

Figure S21. Digital photo of **Cu_3** complexes (concentration: 2×10^{-4} M) in mixed solvents of tetrahydrofuran and ethanol with different f_e under UV light, excited at 365 nm.

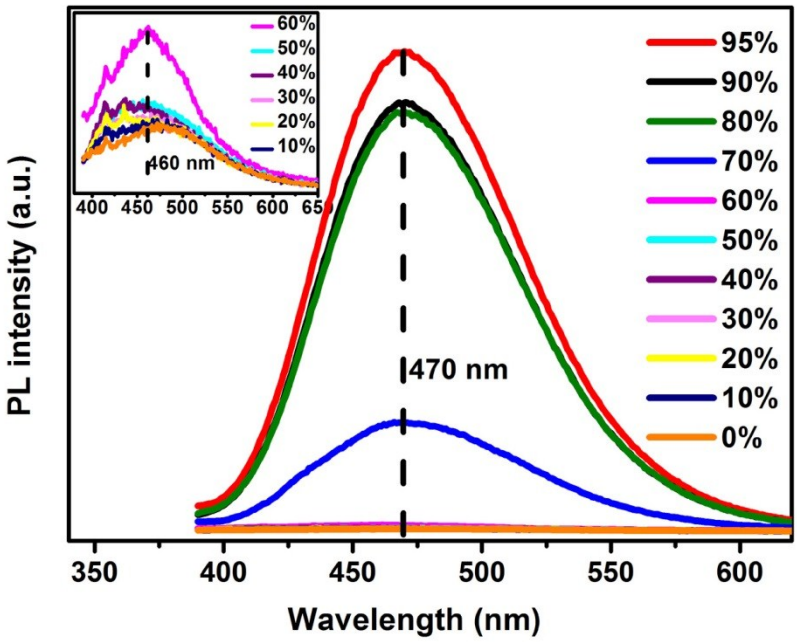

Figure S22. Photoemission spectra of **Cu_3** in mixed solvents with different isopropanol fraction from 0% to 95% (concentration: 2×10^{-4} M), excited at 372 nm.

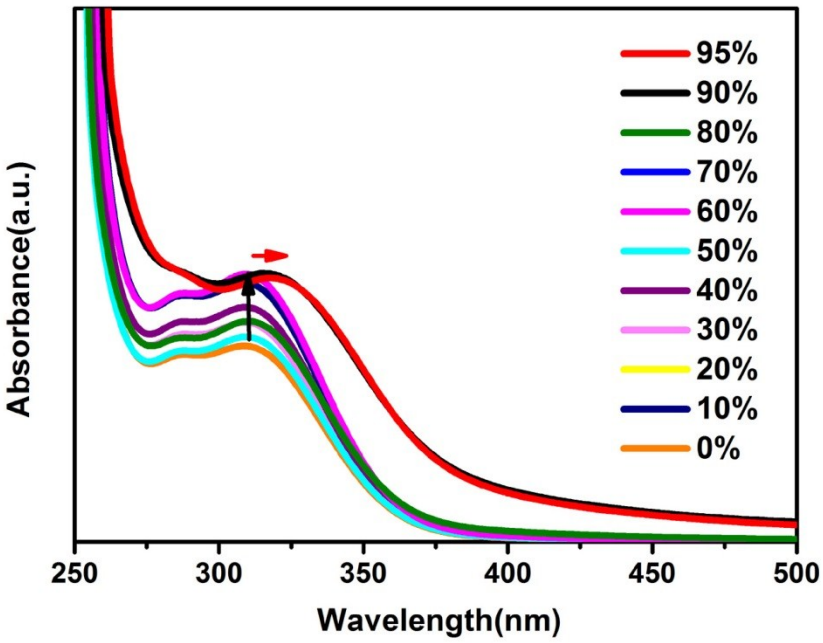

Figure S23. UV−vis absorption of **Cu_3** in mixed solvents with different isopropanol fraction from 0% to 95% (concentration: 2×10^{-4} M), using a 1 mm thickness cuvette.

Crystallographic data

Table S1. Crystal data and structure refinement for **Au_3**, **Ag_3** and **Cu_3.**

	Au_3	**Ag_3**	**Cu_3**
Empirical formula	$C_{98}H_{84}N_6Cl_5Au_3$	$C_{98}H_{83}N_6Cl_6Ag_3$	$C_{98}H_{83}N_6Cl_6Cu_3$
Formula weight	2113.92	1881.07	1748.1
Temperature/K	293(2)	200(10)	149.99(10)
Crystal system	triclinic	triclinic	monoclinic
Space group	*P*-1	*P*-1	$P2_1/n$
a/Å	9.1649(5)	9.0044(3)	9.61574(16)
b/Å	17.6824(5)	17.5149(6)	52.1775(11)
c/Å	29.9758(5)	30.0739(8)	17.2889(3)
α/°	72.855(2)	73.420(3)	90
β/°	87.796(3)	88.480(3)	101.7328(16)
γ/°	76.607(3)	78.205(3)	90
Volume/Å3	4513.4(3)	4447.2(3)	8493.0(3)
Z	2	2	4
ρcalcg/cm^3	1.405	1.226	1.366
μ/mm^{-1}	9.324	0.699	3.003
F(000)	1872.0	1680.0	3604.0
Crystal size/mm^3	0.05 × 0.05 × 0.02	0.05 × 0.05 × 0.03	0.05 × 0.05 × 0.03
Radiation	CuKα (λ = 1.54184 Å)	MoKα (λ = 0.71073 Å)	CuKα (λ = 1.54184 Å)
2θrange for data collection/°	5.354 to 147.332	4.242 to 58.416	5.488 to 134.988
Index ranges	-11 ≤ h ≤ 11, -17 ≤ k ≤ 21, -37 ≤ l ≤ 36	-12 ≤ h ≤ 12, -22 ≤ k ≤ 23, -33 ≤ l ≤ 40	-10 ≤ h ≤ 11, -58 ≤ k ≤ 62, -20≤ l ≤ 20
Reflections collected	36330	55550	44209
Independent reflections	16957 [R_{int} = 0.0776, R_{sigma} = 0.0918]	19998 [R_{int} = 0.0995, R_{sigma} = 0.1708]	15225 [R_{int} = 0.0583, R_{sigma} = 0.0595]
Data/restraints/parameters	16957/24/952	19998/0/952	15225/99/1087
Goodness-of-fit on F^2	0.959	0.929	1.035
Final R indexes [I>=2σ (I)]	R_1 =0.0753, wR_2 = 0.1986	R_1= 0.0648, wR_2= 0.1199	R_1 = 0.0691, wR_2 = 0.1614
Final R indexes [all data]	R_1 = 0.0945, wR_2 = 0.12188	R_1 = 0.1559, wR_2= 0.1422	R_1 = 0.0867, wR_2 = 0.1681
CCDC	1881605	1881607	1881606

$R_1 = \sum||F_o|-|F_c||/\sum|F_o|$. $wR_2 = [\sum w(F_o^2 - F_c^2)^2/\sum w(F_o^2)^2]^{1/2}$

Supplementary References

[1] C. Liu, Y. Hang, T. Jiang, J. Yang, X. Zhang, J. Hua *Talanta*, 2018, **178**, 847–853.

[2] G. Liu, S. Tian, C. Li, G. Xing, L. Zhou *ACS Appl. Mater. Interfaces*, 2017, **9**, 28331−28338.

[3] P. Duan, Z. Wang, J. Chen, G. Yang R. G. Raptis *Dalton Trans.,* 2013, **42**, 14951–14954.

[4] S. Wang, C. Kong *Acta Cryst.,* 2011, **67**, o3199.

[5] CrysAlisPro 2012, Agilent Technologies. Version 1.171.36.31.

[6] G. M. Sheldrick, A short history of *SHELX*. *Acta Cryst.* 2008, *A* **64**, 112–122.

[7] O. V. Dolomanov, L. J. Bourhis, R. J. Gildea, J. A. K. Howard and H. Puschmann, *J. Appl. Cryst.* 2009, **42**, 339–341.

[8] G. M. Sheldrick, Crystal structure refinement with *SHELXL*. *Acta Cryst.* 2015, *C* **71**, 3–8.

[9] A. L. Spek, *Acta Cryst.* 2015, *C* **71**, 9–18.